ELSEVIER

Biochimica et Biophysica Acta 1459 (2000) 218–229

BIOCHIMICA ET BIOPHYSICA ACTA
BBA

www.elsevier.com/locate/bba

A new microsystem for automated electrorotation measurements using laser tweezers

Christoph Reichle [a], Thomas Schnelle [b], Torsten Müller [a], Thomas Leya [a], Günter Fuhr [a,*]

[a] *Lehrstuhl für Membranphysiologie, Institut für Biologie, Humboldt-Universität zu Berlin, Invalidenstr. 42, 10115 Berlin, Germany*
[b] *EVOTEC BioSystems AG, c/o Institut für Biologie, Invalidenstr. 42, 10115 Berlin, Germany*

Received 24 January 2000; received in revised form 24 May 2000; accepted 30 May 2000

Abstract

We have developed a new microsystem for fast, automated studies of reactions and kinetics of single cells with biochemical or pharmacological agents. A cell spins in an external rotating electric field and the frequency dependence characterises the passive dielectric properties of membrane and cytoplasm. We use a planar microelectrode chip with microchannel (easily covered with a removable slip) for the application of frequencies exceeding 250 MHz to determine cytoplasmic properties in low and high conductivity electrolyte solutions. The laser tweezers serve as a bearing system, rotation is induced by microelectrodes and rotation speed is recorded automatically. This opens up new possibilities in biotechnology, e.g. for drug screening as demonstrated by measuring the influence of ionomycin on the passive dielectric properties of T-lymphoma cells. Additionally, a possible infrared-induced long-term cell damage could be observed by electrorotation and is discussed.

Keywords: Electrorotation; Microsystem; Laser tweezers; T-lymphoma cell; Infrared-induced cell damage

1. Introduction

Non-contact methods for single cell handling and manipulation, such as laser tweezers [1,2] or dielectrophoretic field cages (DFC) [3], combined with miniaturised equipment [4] for cell analysis are a growing field of biotechnology. Fast, automatic studies of reactions and kinetics of single cells with biochemical or pharmacological agents are of great interest. One tool is electrorotation (the frequency dependence of cell spinning in an external rotating hf electric field). It can characterise the passive dielectric properties of cell membrane and cytoplasm [5–14]. A combination of laser tweezers and DFCs has been recently described [15,16]. In one application, electrorotation (ER) was successfully used in order to characterise the electric field distribution in a DFC [16].

Here, we introduce a planar microelectrode chip with microchannel that can easily be covered with a removable microscope slide, capable of working with high aperture objectives. The system is compatible with laser tweezers, easy to handle and convenient for the application of frequencies exceeding 250 MHz (necessary to determine cytoplasm properties in low and high electrolyte solutions [11,14]).

* Corresponding author. Fax: +49-30-2093-8635;
E-mail: guenter.fuhr@rz.hu-berlin.de

0005-2728/00/$ – see front matter
PII: S0005-2728(00)00150-X

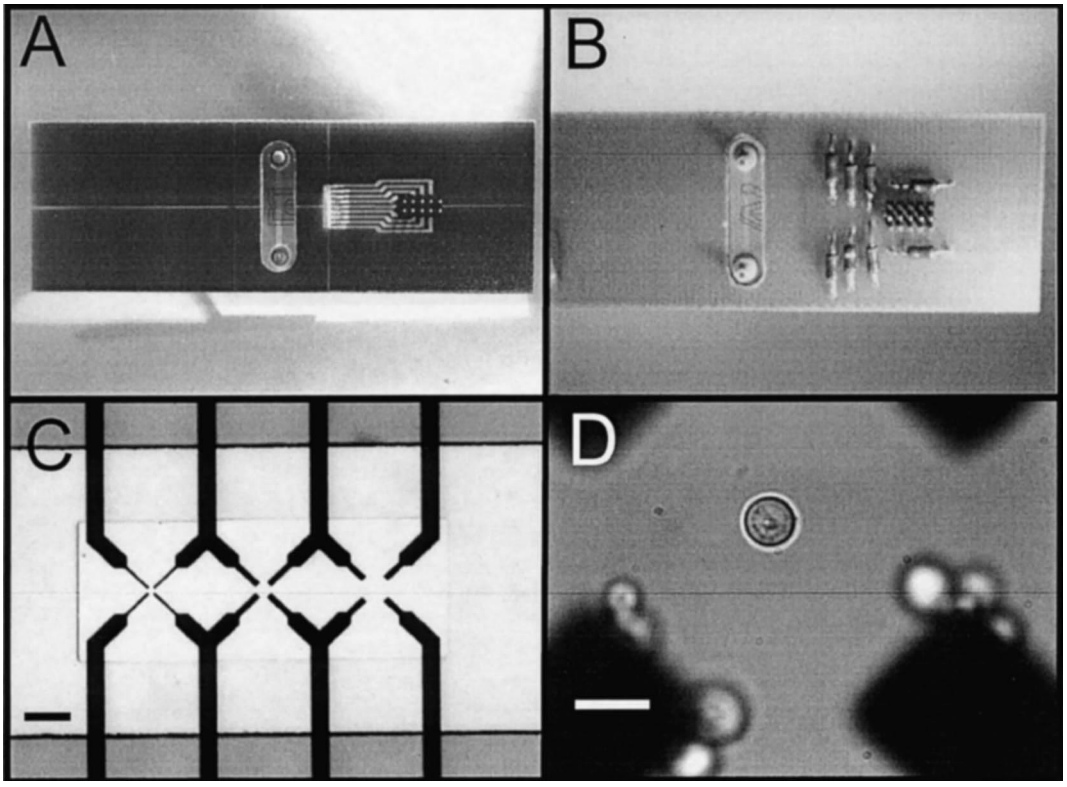

Fig. 1. (A) Picture of the microsystem compatible with laser tweezers. The glass chip with microelectrodes was fixed on a circuit board with the same size as a microscope slide (25×75 mm). (B) Reverse side of the microsystem with fluidic adapter and 50 Ω resistors on the circuit board. (C) Central part showing the three quadrupole traps with 20 μm, 40 μm and 80 μm electrode distance in order to measure differently sized particles and the microchannel (bar = 150 μm). (D) Laser-trapped yeast cell within the 40 μm quadrupole under positive dielectrophoresis (pDEP) conditions ($\sigma = 1.1$ mS m^{-1} and 10 kHz $< f <$ 15 MHz). Except for the trapped yeast in the middle of the electric field trap, cells are attached to the electrodes by positive DEP (bar = 5 μm).

The optical trap positions a particle, while rotation is induced by microelectrodes and the speed is recorded automatically. This opens up some new possibilities for automated electrorotation measurements. As an example, we describe testing the influence of ionomycin on the passive dielectric properties of T-lymphoma cells. Potential photodamage of cells by the Nd:YAG laser is discussed.

2. Materials and methods

2.1. Tweezers-compatible microchip

The microsystems are manufactured by photolithography on planar 500 μm thick glass chips. Twelve electrodes (Ti/Pt: 20/120 nm) are arranged to form three tetrodes with 20, 40 and 80 μm electrode spacing (see Fig. 1C). A 32 μm thick polymer spacer is fixed on this glass plate (14×25 mm) to form a microchannel of 1 mm width and 15 mm length. At both ends of the channel, holes are drilled through the glass substrates. Input and output connections, fixed outside, allow a particle or cell suspension to stream through the chip. The glass chip is fixed to a circuit board with the same size as a microscope slide (25×75 mm) carrying the electric connections (see Fig. 1A). In order to use the microstructure for frequencies above 20 MHz, each of the four generator outputs is grounded on the circuit board through 50 Ω resistors in the immediate vicinity of the chip (see Fig. 1B). Images of the system are shown in Fig. 1.

2.2. Microparticles, cells and media

Air-dried crosslinked dextran spheres (Sephadex G15, Pharmacia, Uppsala, Sweden) were incubated

in distilled water for about 1 h. The beads were filtered through a net with 40 μm mesh size. The particles were diluted in distilled water adjusted to the required conductivity by the addition of phosphate buffered saline (PBS, Biochrom, Berlin, Germany) [11,14].

Yeast cells (*Saccharomyces cerevisiae*, strain Epernay, obtained from Prof. R. Ehwald, Humboldt University Berlin) were harvested with a sterilised needle from the agar petri dish and transferred to a solution of 0.3 M inositol. Afterwards, the yeast cells were fixed with glutaraldehyde (2.5%, Sigma, St. Louis, MO, USA). A cell suspension with a density of about 0.01% was used for experiments. The resulting medium conductivity was 1.1 mS m^{-1}.

T-lymphoma cells (Jurkat and RMA) were grown in RPMI 1640 medium (Gibco Life technologies, Karlsruhe, Germany) containing 10% foetal calf serum, penicillin and streptomycin at 100 IU/ml each (Seromed/Biochrom, Berlin, Germany). They were washed twice with PBS solution prior to use. Cells and particles were centrifuged for 5 min at 2400 rpm (Biofuge, Heraeus Instruments, Germany).

Red blood cells (obtained by needle puncture from a healthy donor) were suspended in PBS. In this medium the erythrocytes were diluted to a haematocrit of 0.01%.

Non-motile, vegetative cells of a coccal green alga (unspecified, held at culture collection CCryoHUB strain no. 001d-99) were used. For growth experiments under continuous laser exposure and continuous spinning assays the coccal green alga *Chlorococcum minutum* Starr 1955 (CCryoHUB 093-99; held as synonym *Chlorococcum sphacosum* Archibald et Bold 1970 at SAG 66.80) was used. Algae were cultured on agar plates with Bold's basal medium [17] or PFW medium [18] under 16:8 h light:dark conditions and at 20°C room temperature. For all experiments algal cells were suspended in the corresponding liquid medium (pH 5.5–6, conductivity 30–80 mS m^{-1}). Postcultures were performed under the microscope at room temperature and under continuous light.

2.3. Single beam gradient trap

The single beam gradient trap (optical tweezers or optical trap) consists of a single strongly focused laser beam [1]. The principle of single beam gradient traps is summarised in the article of Ashkin [2]. The gradient forces F_G, pulling particles towards the focus, have to be dominant above the scattering forces F_S, trying to push particles away from focus in the incident light direction. Thus, the absolute magnitude of the total force is calculated as $F=(F_S^2+F_G^2)^{1/2}$ depending on the angle of beam to particle surface incidence [2].

The incident momentum of the laser beam per second is $F \approx n_1 P/c$ where n_1 is the index of refraction of the fluid surrounding of the sphere, P is the power of the incident ray, and c is the speed of light. For the power, typically used for our experiments (35 mW), one obtains force values in the picoNewton range. This is sufficient to hold a 10 μm particle against streaming velocities up to 50 μm/s or dielectric forces used in our DFCs [15].

For these experiments, we used laser tweezers (P.A.L.M. GmbH, Bernried, Germany) consisting of an inverted microscope (IX 70, Olympus, Germany) and 1 W Nd:YAG laser (TEM_{00}, 1064 nm, LD 3000i, Laser Quantum Ltd., Manchester, UK). To avoid optical damage to the trapped object, infrared beams (e.g. $\lambda = 1064$ nm) are commonly used [19]. The laser is coupled to the epifluorescence path of the microscope and focused with a 100× oil immersion objective (UPlanFl 100×/1.3 oil, Olympus). The microobject behaviour was monitored with a CCD camera (JAI 2040, Protec, Japan). The beam power was determined by a direct objective-to-power measurement in air (Fieldmasters models FM with LM-2, Coherent, USA). This method is incorrect through total internal reflection errors as verified by König et al. [20] and Liang et al. [21]. Therefore, the laser power in situ has to be multiplied by an empirically derived correction factor of about 1.5–1.75. In our case the measured value of laser power was about 35 mW behind the microscope objective. The principle of combined laser trap and microelectrode design is shown in Fig. 2.

2.4. Microoptical single particle dynamics (MOSPAD) detector

By detecting the modulation of light intensity, the angular velocity ω_p of an inhomogeneous structured particle or cell for each applied frequency was ana-

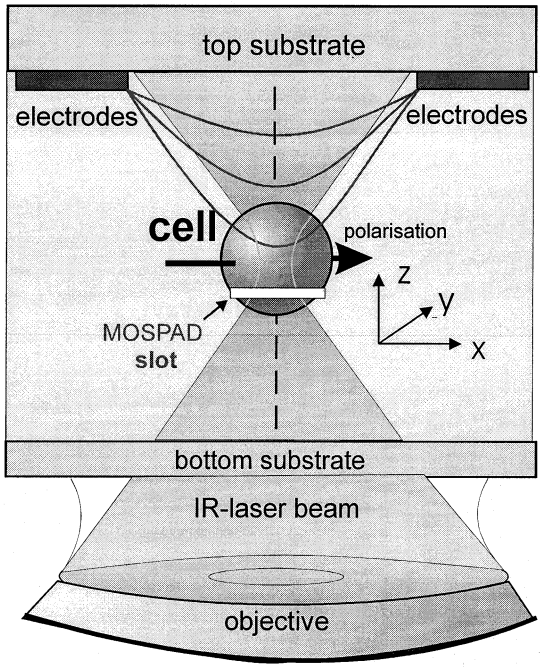

Fig. 2. Side view of the microsystem, designed for electrorotational studies with microchannel. Due to the accurate and stable cell positioning in the focus of the laser beam, the rotation can be recorded automatically. Four Pt electrodes (distance 40 μm) are 90° phase shifted to obtain a rotating field. The flow in the microchannel is horizontal and the optical detection of the cell and particles dynamics is aligned with the beamline of the microscope. For correct optical operation, the bottom glass substrate must be less than 200 μm. By rotating the inhomogeneous structured cell and by observing only a sub-area (here: slot) of it, a modulation of light intensity is converted by a photodiode.

lysed. We used a mask (here slot) within the beam line of the microscope, in order to detect only a subarea of the cell. The modulation of light was converted to a voltage signal by a 'silicon PIN photodiode' (Hamamatsu, Germany) with an amplification of 10^{10} V A^{-1}. Only one rotation of the cell is sufficient, since the peak to peak time is calculated. For more information about the automatic detection of single particle rotation speed, see Reichle et al. [22].

2.5. Set-up, field generation and automation

A four phase (90°, square wave, duty cycle 50%) pulse generator (HP 8131 A, Hewlett Packard, USA) with a frequency range of 0.0001–250 MHz produced the rotating field. The laboratory written software controlled the applied frequency in logarithmic steps and analysed the output of the MOSPAD detector. The height of the particle within the microchannel was controlled with a micrometer adapter (MT 12, Heidenhain GmbH, Traunreut, Germany). The standard deviation of height measurements was about ±1 μm. A schematic diagram of the experimental setup is shown in Fig. 3. About 10–15 μl of the suspension was pipetted into the microchannel. Thin layers of silicone grease on the polymer spacer were used to seal the coverslip. Trapping was performed through this coverslip window. All measurements were carried out at a room temperature of 23°C. The conductivity of media was measured with a conventional two-electrode conductometer (WTW, LF 325, Weilheim, Germany).

3. Theory

Using dipole approximation, the time averaged dielectrophoretic force $\overrightarrow{F}$, acting on a suspended dielectric cell or particle of radius R, in a time periodic field E, with radian frequency ω, can be expressed as:

$$\langle \overrightarrow{F} \rangle = 2\pi\varepsilon_1 R^3 \left[Re(f_{CM}) \cdot \overrightarrow{\nabla} E_{rms}^2 + Im(f_{CM}) \cdot \left(\sum_{\mu,\nu} \left[E_\mu^{re} \frac{\partial E_\mu^{im}}{\partial \upsilon} - E_\mu^{im} \frac{\partial E_\mu^{re}}{\partial \upsilon} \right] \overrightarrow{e}_\upsilon \right) \right] \quad (1)$$

with μ, $\nu = x, y, z$ and the unit vector $\overrightarrow{e}$. The Clausius–Mossotti factor f_{CM} reflects the dielectric properties of a homogeneous sphere (index p) in surrounding liquid (index l) [23].

$$f_{CM} = \frac{\tilde{\sigma}_p - \tilde{\sigma}_l}{\tilde{\sigma}_p + 2\tilde{\sigma}_l} \quad (2)$$

with the complex conductivity $\tilde{\sigma} = \sigma + i\omega\varepsilon_0\varepsilon$. There σ and ε stand for static conductivity and absolute permittivity, respectively.

The torque is given by

$$\langle \overrightarrow{N} \rangle = 4\pi\varepsilon_1 R^3 \, Im(f_{CM}) \, \overrightarrow{E}^{im} \times \overrightarrow{E}^{re} \quad (3)$$

The nature of particles (single- or multi-shelled, spherical or ellipsoid) can be taken into account [24,25]. In general, each relaxation process (e.g. at

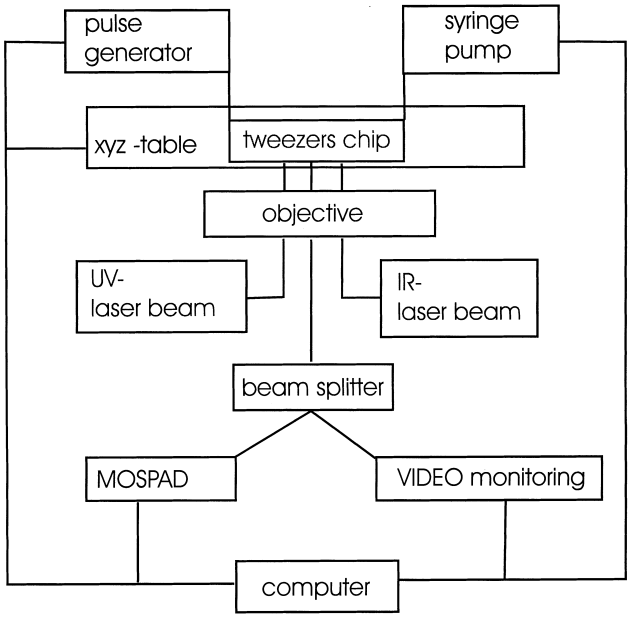

Fig. 3. Scheme of the experimental set-up to obtain automatic electrorotational spectra of cells or artificial particles.

the interface or due to dispersions of cell compartments) can yield one electrorotational peak [11,26].

The effective complex particle conductivity for e.g. a single-shelled sphere is given by

$$\tilde{\sigma}_p = \tilde{\sigma}_m \left\{ \frac{a^3 + 2\left(\frac{\tilde{\sigma}_c - \tilde{\sigma}_m}{\tilde{\sigma}_c + 2\tilde{\sigma}_m}\right)}{a^3 - \left(\frac{\tilde{\sigma}_c - \tilde{\sigma}_m}{\tilde{\sigma}_c + 2\tilde{\sigma}_m}\right)} \right\} \quad (4)$$

with $a = R/(R-h)$ and shell (membrane) thickness h. The indices c and m refer to cytoplasm and membrane, respectively. Further shells can be considered iteratively. For biological cells, the assumption of homogeneous compartments is not generally justified. The cytoplasm often contains organelles or vacuoles. For example, in the cell interior of mammalian erythrocytes, the resulting conductivity and permittivity may show a frequency dependence due to, e.g. Debye relaxation processes of solved globular proteins in the MHz range and of bound and free water molecules in the upper MHz range and near 20 GHz, respectively. This gives rise to the following general expression for conductivity and permittivity of each compartment [14]:

$$\sigma = \sigma_0 + \sum_{k=1}^{n} \Delta\sigma_k \frac{(\omega\tau_k)^2}{1 + (\omega\tau_k)^2} \quad (5)$$

$$\varepsilon = \varepsilon_\infty + \frac{1}{\varepsilon_{vac}} \sum_{k=1}^{n} \frac{\tau_k \Delta\sigma_k}{1 + (\omega\tau_k)^2} \quad \Delta\varepsilon = -\tau\Delta\sigma \quad (6)$$

where ε_{vac}, ε_∞, σ_0, σ_∞, $\Delta\sigma$, $\Delta\varepsilon$ and τ represent the low and high frequency limit of permittivity, static conductivity, conductivity increment, permittivity decrement due to dispersion and relaxation time for n different relaxation processes.

4. Results and discussion

4.1. Electric field distribution

Due to the complex electrode geometry and boundary conditions, there is no analytic solution for the electric field distribution in the planar four electrode structures. Therefore, a finite difference method [27] was used to solve the complex field equation: (for details see [3,28]).

$$\nabla[(\sigma + i\omega\varepsilon)\nabla\phi] = 0 \text{ with } \vec{E} = -\nabla\phi \quad (7)$$

In a planar four-electrode chamber driven with rotating electric fields, dielectric particles showing negative dielectrophoresis are centred due to horizontal field gradients inside the trap. Additionally, there are strong vertical gradients resulting in particle levitation. Therefore, particles would leave the trap at higher voltages (see Fig. 4A). Velocity of particle rotation depends on the field frequency, the dielectric properties and the local electric field strength. Thus, for automatic measurements of ER spectra, it is necessary to fix the object, e.g. by laser tweezers on the central vertical axis of the trap.

The dependence of rotation speed on height above the electrode plane in this axis is shown in Fig. 4B for the 80 μm trap. For a large enough distance from the electrode plane, the experimental values fit the numerical expectation (solid line). Near the surface of about 7.5 μm, the spinning velocity of a particle of about 5 μm in diameter is reduced due to the increased friction (dotted line). This gives the opportunity to measure hydrodynamic drag near surfaces. For reliable measurements of ER spectra, a particle

should be separated from the surface by about twice its diameter.

4.2. Shadowing effect

Using laser tweezers in microchambers with electrodes on the bottom substrate, we observed a 'shadowing effect' when the trapped particle is out of the centre of the chamber. This feature can be understood using a ray optics model of the trapping force. When the TEM_{00} Nd:YAG laser beam is shadowed by the electrode area, a virtual higher-order mode (e.g. TEM_{03}) is created. Thus, the asymmetric trapped red blood cell is inserted into the shaped laser beam. By shifting the height of the cell regarding the electrode plane, a slip into the virtual mode can be observed in about 10 μm height (see Fig. 5).

This effect only appears in chambers with electrodes on the bottom side, as in an octode geometry

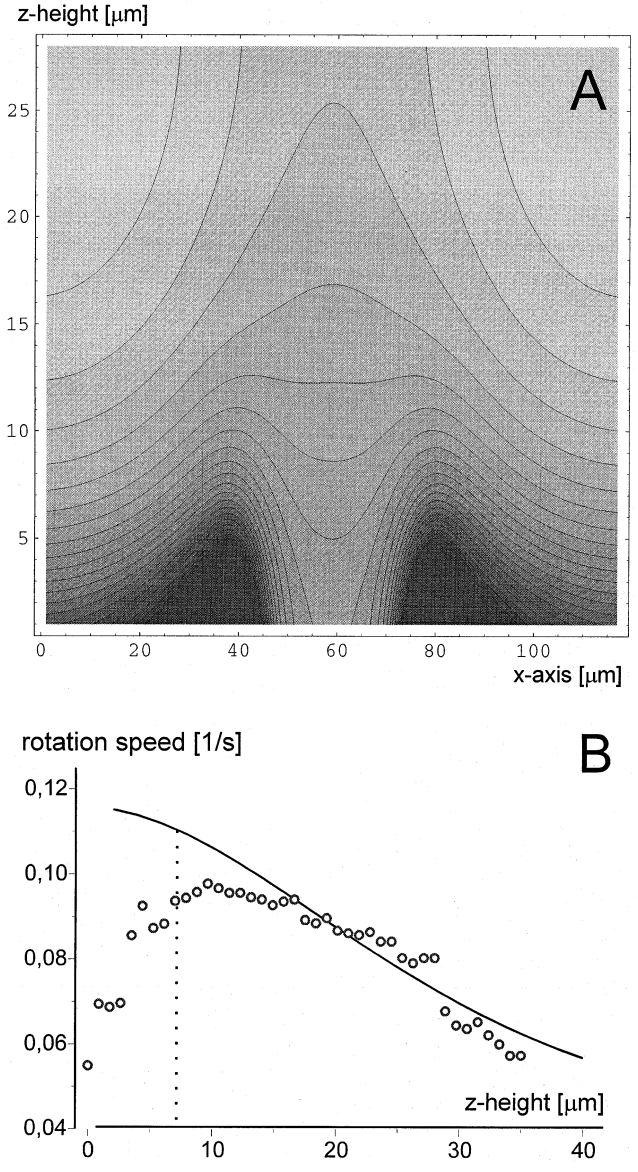

Fig. 4. (A) Numerical result for symmetric quadrupole trap with contour plot of mean square electric field (potential of dielectrophoretic force) in the xz plane. The electrode distance is 80 μm. (B) Inverse rotation speed of yeast ($\sigma = 1.1$ mS m^{-1} and $f = 1$ MHz) in the central vertical axis. The fit represents the z component of dielectric torque.

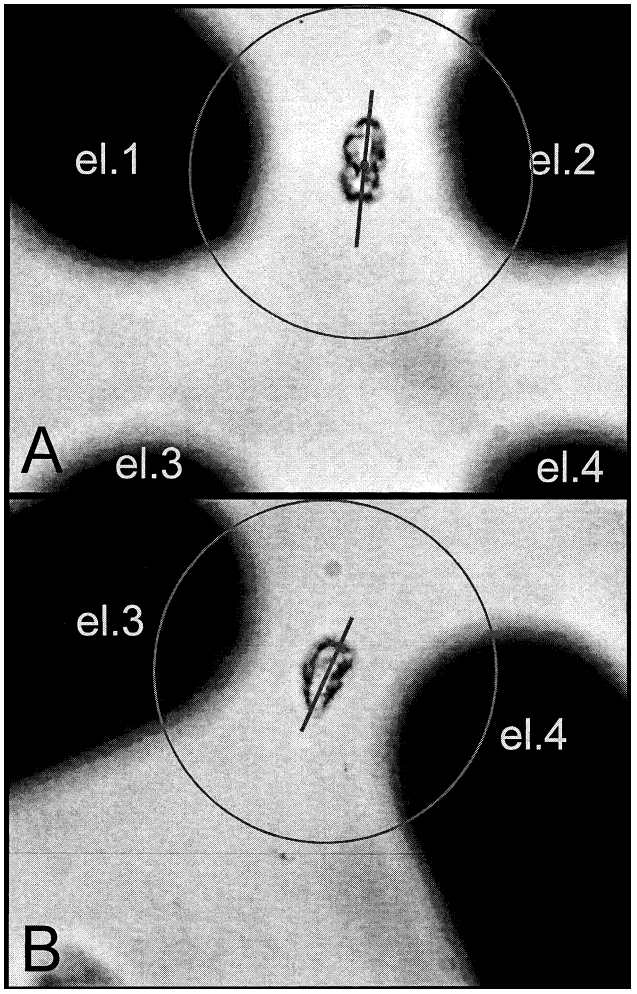

Fig. 5. Red blood cell (echinocyte) trapped with tweezers at a height of 10 μm above a bottom electrode plane ($\sigma = 1.5$ S m^{-1}). The circle represents the diameter of the laser beam (30 μm) in electrode plane. (A) The trapped red blood cell was inserted into the shaped laser cone. (B) Shifting the microelectrode structure through an angle of about 15° leads to a simultaneous twist of the red blood cell.

Table 1
Fitted parameters (passive dielectric properties) of measured cells and particles

	Membrane		Cell or particle interior					
	ε_∞	σ_0 (10^{-6} S m^{-1})	ε_∞	σ_0 (S m^{-1})	$\Delta\sigma_1$ (S m^{-1})	$f_1 = 2\pi/\tau_1$ (MHz)	$\Delta\sigma_2$ (S m^{-1})	$f_2 = 2\pi/\tau_2$ (MHz)
Sephadex particle (A)	–	–	40	0.00065	0.001	2	0.00014	120
Yeast cell (B)								
Double-shelled	60	10^4	50	0.19	–	–	–	–
	8	100	–	–	–	–	–	–
Jurkat cell (C)								
Reference control	6	3	45	0.4	0.25	7	0.12	70
Jurkat cell (D)								
(a) 1 μM ionomycin	8	30	63	0.4	0.2	2	0.3	20
(b) 10 μM ionomycin	8	30	75	0.45	0.4	2	0.3	30
Jurkat cell (E)								
(a) 10 min	4	3	35	0.25	0.125	4	0.175	40
(b) 20 min	4	3	40	0.35	0.1	4	0.175	40
(c) 40 min	4	3	60	0.62	0.1	4	0.25	40
Green alga (F)	9	5	75	0.4	–	–	–	–

[16]. Thus, the presented microsystem has the advantage of having its electrodes on the top side (see Fig. 2) in order to avoid any shadowing effect.

4.3. Electrorotational measurements

We tested the complete computer-controlled set-up with several cells and particles for compatibility with automation from several kHz up to 250 MHz. The rotation speed was analysed automatically with the MOSPAD detector [22]. The time needed for measuring 40 rotation speeds per spectrum was roughly 5 min (or about 7.5 s for a single data point).

The accuracy for determining the rotation time for artificial particles was up to 0.02 s. This is achieved by a good reproducibility of artificial particle rotation and thus by the good periodicity of the scattered light.

For cells, the situation is different. Small changes of the rotation axis (due to the inhomogeneous character of the cytoplasm and the non-spherical geometry) and movement of the lymphoma cell's filopodia may slow down or speed up the induced electrorotation. Although the MOSPAD detector works in the same manner as with artificial particles, the cell itself causes small perturbations in the periodicity of the rotation speed of < 0.2 s. Fig. 6 shows several spectra for positive and negative dielectrophoresis. Fitted parameters are in Table 1.

4.3.1. Artificial particles

The Sephadex particle demonstrates the efficiency of the new microsystem for electrorotation measurements using laser tweezers (see Fig. 6A). The good agreement of numeric fit and measured data points shows that chamber resonance [14] is not disturbing the rotation measurements up to 250 MHz. (The chamber has a resonance at 630 MHz which amplifies the third harmonic of a 210 MHz [11] signal but this has no effect on the dielectric parameter fit.)

As a second test, we used glutaraldehyde fixed yeast cells and measured three spectra in 20 min each (see Fig. 6B). The yeast cells stayed stable for more than 40 min. The small shift of the last spectrum toward higher frequencies was probably due to a slight increase of the outer medium conductivity by ($\sigma = 1$ mS m^{-1}). Changes in rotation velocity or spectra would therefore be due to changes in the passive dielectric properties of the cell's compartments.

4.3.2. T-lymphoma cells

The influence of ionomycin on the passive dielectric properties of a human T-lymphoma cell (Jurkat) was tested by electrorotation. Ionomycin (10 μM) causes a large increase in the cytosolic free [Ca^{2+}] concentration [29] and thus leads to damage of the cell. Three untreated cells as reference value were measured (see Fig. 6C). The addition of 10 μM as well as 1 μM ionomycin leads to an acceleration of

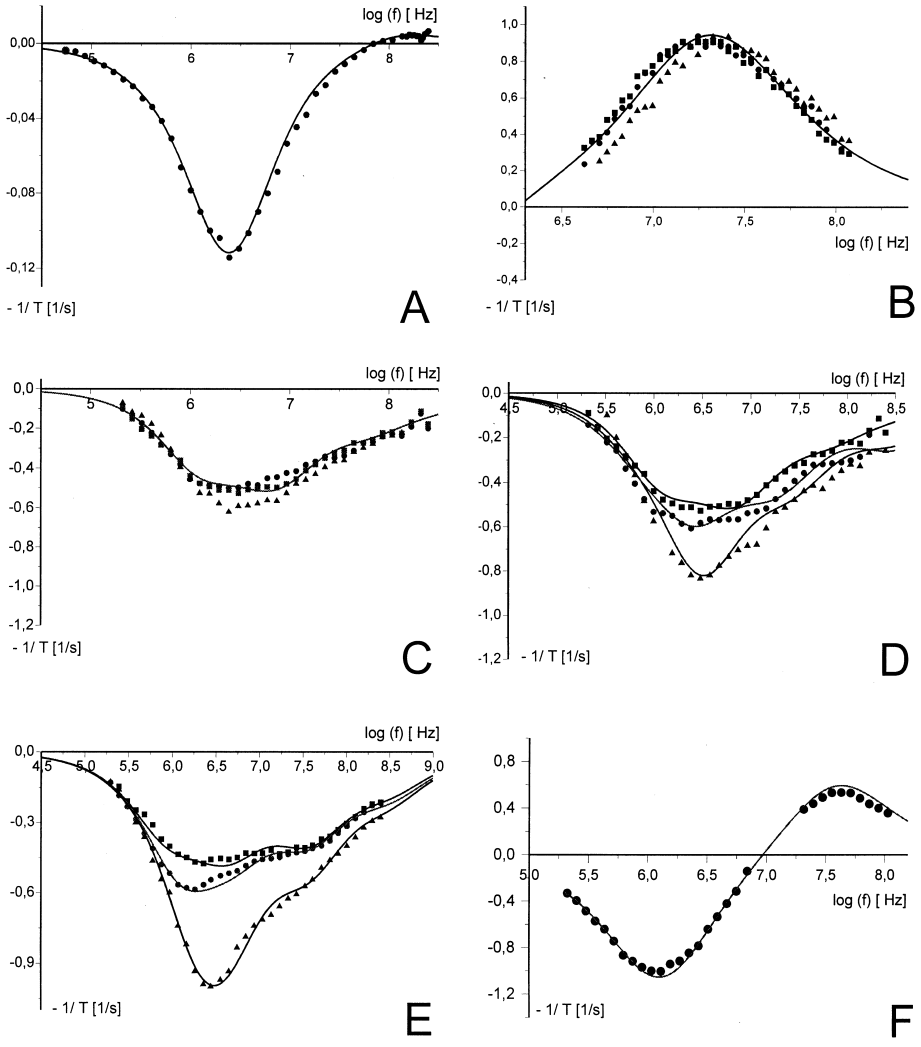

Fig. 6. Electrorotational spectra of cells and artificial particles trapped by laser tweezers in the middle 40 μm electrode trap. (Fit parameter are shown in Table 1). (A) Spectrum of Sephadex particle under nDEP conditions (in water of 13 mS m^{-1}, laser power 35 mW, U_{rms} = 0.6 V). The particle diameter was 35 μm. (B) Spectrum of yeast under positive DEP conditions (in water of 1.1 mS m^{-1}, laser power 35 mW, U_{rms} = 0.4 V). Curve (●) was measured at the beginning, curve (■) after 20 min and curve (▲) after 40 min. The yeast was modeled as a two-shell sphere: 200 nm cell, 8 nm membrane, diameter of sphere was 5 μm. (C) Three reference spectra (●, ■, ▲) of a T-lymphoma (Jurkat) cell in PBS solution at 1.5 S m^{-1} (laser power 35 mW, U_{rms} = 0.4 V). The cell was simulated as a shelled sphere with dispersion of the cytoplasm, whereas the representative fit corresponds to the (■) curve. (D) Spectrum of a T-lymphoma (Jurkat) cell in PBS solution at 1.5 S m^{-1} (laser power 325 mW, U_{rms} = 0.4 V) (■). The addition of 1 μM (●) or 10 μM (▲) ionomycin leads to an acceleration of the cell. The cell was simulated as a shelled sphere with dispersion of the cytoplasm. (E) Spectrum of a T-lymphoma (RMA) cell in PBS solution at 1.5 S m^{-1} (U_{rms} = 0.4 V) (■). An influence of the laser tweezers after 20 min (●) and 40 min (♦) is observed. (F) Spectrum of a green alga in water at 11 mS m^{-1} (laser power 15 mW, U_{rms} = 1.3 V). The green alga was simulated as a double-shelled particle with cell wall, membrane and interior.

the cells spinning in the MHz range (Fig. 6D). The fitting of the spectra indicates an increase of the cytoplasm conductivity from 0.8 to 1.15 S m^{-1}. This is the important parameter for the 10 μM solution.

The reduced hindrance of the ions within the cytoplasm by a factor of 3 is caused by an incorporation of solution and a simultaneous increase of the cell volume. Thus, the apparent inner conductivity increases up to the value of the outer solution. Nevertheless, by measuring the cells within a low outer conductivity, the apparent dielectric conductivity of the cytoplasm would decrease due to leakage

of the cell. Due to the overlay of inner conductivity changes to the changes of the membrane conductivity, values between 10^{-7} and 10^{-6} are not resolvable.

Mouse T-lymphoma cells (RMA) were measured after 10, 20 and 30 min in order to observe a possible influence of the laser beam. The analysis of complete rotational spectra of Jurkat (see Fig. 6E) also showed an acceleration especially in the MHz range. Spectrum simulation leads to the conclusion that similar to the ionomycin effect an increase of the cytoplasm conductivity from 0.5 (■) to 0.8 (●) to 1.5 S m^{-1} (▲) can be observed. For RMA cells, rotating at similar electric field strengths in a planar four-electrode chamber without trapping with the laser beam, no change in spinning velocity over about 20 min could be observed. Parallel investigations with fluorescence correlation spectroscopy showed no incorporation of propidium iodide [30].

4.3.3. Coccal green alga (CCryoHUB 001d-99)

A rotation spectrum of the coccal alga is shown in Fig. 6F. Spinning at constant speed for the same alga can be ensured for up to 60 min ($f=2$ MHz, $U_{rms}=2.7$ V, laser power $P=35$ mW) *Chlorococcum minutum* (CCryoHUB 093-99/SAG 66.80). To verify that the laser tweezers have no inhibitory influence on growth and development of algal cells, we trapped 10 vegetative cells each for 1, 2, 5 and 10 min (laser power 35 mW) in separate experiments and postcultured them. Development of old vegetative cells into sporangia and release of zoospores was observed within the following 12 h as far as the algae treated for 1, 2 and 5 min and untreated control cells are concerned. Development of the cells treated for 10 min was inhibited (Table 1).

To observe changes in spinning under the influence of the laser beam (see Fig. 6E), we set the applied electric frequency to be fixed at $f=3$ MHz. The control (without laser) showed a nearly constant rotation speed over 20 min. We investigated 10 RMA cells at a laser power of 35 mW, measured after the microscope objective. Three cells showed changes after 6 min, four of them after 13 and the last three after 18 min. Fig. 7D shows a strong acceleration (about 100%) after damaging the membrane directly with a short UV laser pulse ($\lambda=340$ nm). Thus, the

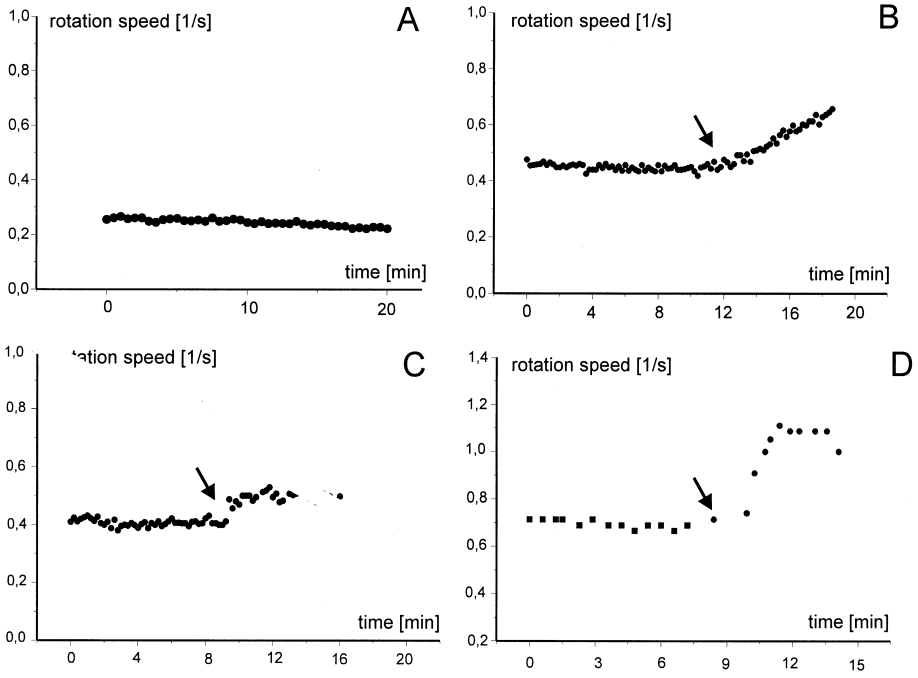

Fig. 7. Different types of kinetics of rotational behaviour during laser trapping (T-lymphoma cell, RMA). (A) Inter-relation of time and inverse rotation time (only rotational electric field). No significant change in the rotation speed could be measured during 20 min. (B) Enhanced rotation speed after 12 min of IR laser trap application ($P=35$ mW). (C) Jump of rotation speed after 9 min of IR laser irradiation. (D) A similar behaviour can be observed by damaging the membrane with a UV laser beam pulse (after 8 min).

acceleration of the spinning may be a sensitive test for damage caused by laser tweezers.

Only a few results about possible damage in IR laser traps are published [19,21,31–34]. They are limited substantially to the following objects: bacteria: *Escherichia coli* [19,33], yeast cells: *S. cerevisiae* [19], red blood cells [19], CHO cells [21,31,32], human spermatozoa [31] and green algae: *Spirogyra* [19] and *Haematococcus pluvialis* [20]. The authors often used different laser power with different calibration procedures and not the incident photon energy at the laser focus. This complicates the evaluation of the cw laser influence. In the following, the mentioned laser power always refers to the laser power in the cited paper.

Reproduction of yeast cells by continuous budding trapped with a cw 1064 nm laser of 80 mW power and up to 5 h was reported by Ashkin et al. [19]. He also found (under similar laser conditions) that reproduction rates for *E. coli* were unaffected. However, Neumann et al. [33] reported a laser wavelength and intensity influence on the transmembrane potential-dependent flagellar rotation of *E. coli*.

Most of the investigations concern CHO cells. Liang et al. [21] found that the cloning efficiency of laser irradiated cells was least at 740–760 nm, good at 800–850 nm and 950–990 nm and moderate at 900 nm and 1064 nm for exposure times of less than 5 min and 88 mW. Schneckenburger et al. [32] only found a slightly lower cell growth and cloning efficiency of CHO cells irradiated with 100 mW for 2 min compared to untreated cells. König et al. [31] reported that CHO cells irradiated with 760 nm (1 min) form no clones whereas a cloning efficiency of 80–50% was measured following 1–10 min IR laser (800 nm) exposure and 5–6 days cultivation. The results strongly suggest that the survival rate is dependent on the wavelength, power density and time. For the cw 1064 nm laser beam the trapping time should not exceed 3 min at 88 mW or 1 min at 176 mW [21]. Electrorotation as a criterion for cell vitality indicates that the manipulation time should be limited to less than 6 min (compare Fig. 7).

Damage-free trapping and manipulation (optical state of the chloroplast and motility) was also reported for the green algae *Spirogyra* (1064 nm, 80 mW, several minutes [19]) and *Haematococcus* (1047 nm, 100 mW, 1 min [20]). In our experiments (1064 nm, 35 mW, 1–5 min) no influence was observed of the optical trap on the development of vegetative coccal green alga into sporangia and the release of zoospores. Only the applying of laser beam up to 10 min stopped the development of vegetative cells. In contrast to the spinning behaviour of the sensitive Jurkat cells the electrorotation of these green algae is constant up to 60 min (Fig. 6F).

Human red blood cells were manipulated using optical tweezers (1064 nm) with no apparent change in flexibility or appearance with powers of 4–40 mW. At a power of about 80 mW some loss of membrane flexibility was observed after more than 10 min [19]. This is in contrast to our experiments where we found clear changes of electrorotational spectra after 6 min (unpublished results). Bronkhorst et al. [35] reported changes of mechanical properties of red blood cells replacing native plasma with PBS. Indeed we incubated the erythrocytes in PBS where some echinocytes were present. The red blood cells are very sensitive to changes of medium solution (protein and electrolyte content). The additional stress of the laser irradiation to red blood cells can reinforce the changing of the passive dielectric properties detected by electrorotation. Two main reasons could be responsible for IR-induced cell damage: interaction of the highly focussed laser beam with various cellular components of the biological cells may result in intracellular heating and one- and two-photon effects induced by photochemical reactions [21].

Liu et al. [36] investigated the temperature increase induced by cw 1064 nm on phospholipid vesicles and on CHO cells. They found a moderate temperature change for both microobjects of about 1.1°C/100 mW of laser power due to the low water absorption on this spectral region. Therefore, the authors did not make the temperature effect responsible for the cw 1064 laser beam-induced trapping damage. The temperature change induced by the electric field is dependent on the power of the field and the conductivity of the outside medium. For the temperature increase in high conductivity solutions such as PBS one finds a temperature increase of 1–2°C. Under permanent field influence cultivated fibroblasts can well tolerate an electric field-induced temperature rise of 2°C at a cultivation temperature up to 37°C [37].

However, the combination of electric field and la-

ser beam can increase the intra- and extracellular thermal convection [20] as recently demonstrated by enhanced fluid rotation in combined 'rotating dielectric field cages/laser tweezers' [16]. Additionally, while spinning the structured and inhomogeneous microparticle may pass through several trap positions. This may induce further mechanical and electrohydrodynamic stress.

Recently, Neumann et al. [33] characterised the trapping damage of *E. coli* for optical trapping in the range 790–1064 nm. The photodamage exhibits minima at 830 and 970 nm and maxima at 870 and 930 nm. Because the effect of photodamage was linearly dependent on the intensity, the authors favour a single photon process. The damage was distinctly reduced under anaerobic conditions [33]. These findings strongly suggest the important role of reactive oxygen species induced by laser irradiation. These free radicals are able to impair the cell viability and subsequent reproduction processes at the level of membrane and DNA. However, especially glutathione and carotenoids in green cells are good protectants against oxidative injury by quenching free radicals. Therefore, the relation of oxygen content and the concentration of antioxidants may influence the degree of damage by optical trapping lasers. The high content of oxygen in red blood cells may result in their sensitivity to laser irradiation and clear changes of electrorotation signal. On the other hand the high content of carotenoid in green algae may protect against these damaging processes. Electrorotation measurements concerning the influence on the cells of antioxidants would lead to a better insight and have to be studied. Furthermore, the cloning efficiency and cell growth of the cells have to be taken into account not only for adhering cells.

5. Conclusions

Optical tweezers are a well accepted tool in molecular and cell biology for trapping and manipulating cells and organelles. We used the laser tweezers for stable positioning of cells and particles within a four-electrode trap. By trapping the particle at a sufficient height (e.g. 10 μm above the surface), undefined adhesion between cell and substrate was suppressed. Exact positioning is achieved over a wide range of applied voltages and frequencies, which is fundamental for the automatic recording of dielectric spectroscopy measurements. The time for measuring one spectrum with 40 rotation speeds was roughly 5 min. Compared to imaging methods [38] this span can be reduced by increasing the applied voltage and thus by an accelerated spinning. Nevertheless, an upper limit is given by the induced transmembrane potential at frequencies in the kHz range. Furthermore, the advantage of the tweezers set-up over an octopole geometry is the possibility to measure the cell at negative and positive dielectrophoresis conditions. Combining laser tweezers and microelectrodes, one should take into account the observed shadowing effect of the IR laser beam at the microelectrodes. This leads to an alignment of asymmetric cells (e.g. red blood cells). Nevertheless, this effect could not be observed outside the centre of the cage (see Fig. 5).

The set-up is convenient for automated and kinetic studies with biochemical or pharmacological agents. The addition of 10 μM ionomycin to human T-lymphoma cells was clearly reflected in an acceleration of the cell in the MHz range and the numeric fit showed an increase in the cytoplasm conductivity. Additionally, possible IR-induced long-term cell damage could be observed by electrorotation. Further experiments in this field should lead to a deeper understanding of IR laser interaction with cells, especially in the growing field of laser tweezers applications in cell and molecular biology.

Acknowledgements

We acknowledge Dr G. Gradl (EVOTEC BioSystems AG, Hamburg) for experimental support with the ionomycin experiments and Dr K. Schütze (P.A.L.M. GmbH, Bernried) for the generous instrumental support. We thank Dr S. Howitz (GeSIM GmbH, Großerkmannsdorf) for fabrication of the microstructures and Dr M. Franke for fabrication of the PIN photodiode and amplifier. We would like to thank Dr K. Sparbier (Charité, Berlin) for preparing the RMA cells. Dr S.G. Shirley's critical reading of the manuscript is gratefully acknowledged. This work was supported by DFG (SCHN

317/6-3, FU 345/7-1), the German BMBF/VDI/VDE to G.F. (16SV657).

References

[1] A. Ashkin, J.M. Dziedzic, J.E. Bjorkholm, S. Chu, Optics Lett. 11 (1986) 288–290.
[2] A. Ashkin, Biophys. J. 61 (1992) 569–592.
[3] Th. Schnelle, R. Hagedorn, G. Fuhr, S. Fiedler, T. Müller, Biochim. Biophys. Acta 1157 (1993) 127–140.
[4] T. Müller, G. Gradl, S. Howitz, S. Shirley, Th. Schnelle, G. Fuhr, Biosens. Bioelectr. 14 (1999) 247–256.
[5] W.M. Arnold, U. Zimmermann, J. Electrostat. 21 (1988) 151–163.
[6] V.Ph. Pastushenko, P.I. Kuzmin, Y.A. Chizmadzhev, Biol. Membr. 5 (1988) 65–78.
[7] G. Fuhr, P. Rösch, T. Müller, V. Dressler, H. Göring, Plant Cell Physiol. 31 (1990) 975–985.
[8] K. Kaler, J. Xie, T.B. Jones, R. Paul, Biophys. J. 63 (1992) 58–69.
[9] Y. Huang, R. Pethig, R. Hölzel, X.B. Wang, Phys. Med. Biol. 37 (1992) 1499–1517.
[10] F.F. Becker, X.B. Wang, Y. Huang, R. Pethig, J. Vykoukal, P.R.C. Gascoyne, Proc. Natl. Acad. Sci. USA 92 (1995) 860–864.
[11] J. Gimsa, T. Müller, Th. Schnelle, G. Fuhr, Biophys. J. 66 (1996) 1244–1253.
[12] J.P.H. Burt, K.L. Chan, D. Dawson, A. Parton, R. Pethig, Ann. Biol. Clin. 54 (1996) 253–257.
[13] V.L. Sukhorukov, M. Mussaurer, U. Zimmermann, J. Membr. Biol. 163 (1998) 235–245.
[14] Th. Schnelle, T. Müller, G. Fuhr, Med. Biol. Eng. Comp. 37 (1999) 264–271.
[15] G. Fuhr, Th. Schnelle, T. Müller, H. Hitzler, S. Monajembashi, K.O. Greulich, Appl. Phys. A 67 (1998) 385–390.
[16] Th. Schnelle, T. Müller, Ch. Reichle, G. Fuhr, J. Appl. Phys. B 70 (2000) 267–274.
[17] H.W. Bischoff, H.C. Bold, Univ. Texas Publ. 6318 (1963) 95.
[18] R.W. Hoham, Syesis 6 (1973) 255–263.
[19] A. Ashkin, J.M. Dziedzic, T. Yamane, Nature 330 (1987) 769–771.
[20] K. König, S. Boehme, N. Leclerc, R. Ahuja, Cell Mol. Biol. 44 (1998) 763–770.
[21] H. Liang, K.T. Vu, P. Krishnan, T.C. Trang, D. Shin, S. Kimel, M.W. Berns, Biophys. J. 70 (1996) 1529–1533.
[22] Ch. Reichle, T. Müller, Th. Schnelle, G. Fuhr, J. Phys. D Appl. Phys. 32 (1999) 2128–2135.
[23] G. Fuhr, U. Zimmermann, S.G. Shirley, in: U. Zimmermann, G.A. Neill (Eds.), Electromanipulation of Cells, CRC Press, Boca Raton, FL, 1996, pp. 259–328.
[24] G. Fuhr, T. Müller, R. Hagedorn, Biochim. Biophys. Acta 980 (1989) 1–8.
[25] A.V. Sokirko, Biol. Membr. 6 (1992) 587–600.
[26] G. Fuhr, P.I. Kuzmin, Biophys. J. 50 (1986) 789–795.
[27] A.R. Mitchell, D.F. Griffiths, The Finite Difference Method in Partial Difference Equations, John Wiley, New York, 1980.
[28] Th. Schnelle, T. Müller, G. Gradl, S.G. Shirley, G. Fuhr, J. Electrostat. 47 (1999) 121–132.
[29] J.B. Smith, T. Zheng, R.M. Lyu, Cell Calcium 10 (1989) 125–134.
[30] G. Gradl, T. Müller, Ch. Reichle, Th. Schnelle, G. Fuhr, Eur. J. Cell Biol. 78 (Suppl. 49) (1999) 220.
[31] K. König, H. Liang, M.W. Berns, B.J. Tromberg, Nature 377 (1995) 20–21.
[32] H. Schneckenburger, A. Hendinger, R. Sailer, M.H. Gschwend, M. Bauer, W.S.L. Strauss, K. Schütze, Proc. SPIE 3197 (1997) 263–267.
[33] K.R. Neumann, E.H. Chadd, G.F. Liou, K. Bergmann, S.M. Block, Biophys. J. 77 (1999) 2856–2863.
[34] K.O. Greulich, Micromanipulation by Light in Biology and Medicine: The Laser Microbeam and Optical Tweezers, Birkhäuser, Basel, 1999.
[35] P.J. Bronkhorst, G.J. Streekstra, J. Grimbergen, E.J. Nijhof, J.J. Sixma, G.J. Brakenhoff, Biophys. J. 69 (1995) 1666–1673.
[36] Y. Liu, K.D. Cheng, G.J. Sonek, M.W. Berns, B.J. Tromberg, Appl. Phys. Lett. 65 (1994) 919–921.
[37] G. Fuhr, H. Glasser, T. Müller, Th. Schnelle, Biochim. Biophys. Acta 1201 (1994) 353–360.
[38] G. De Gasperis, X.B. Wang, J. Yang, F.F. Becker, P.R.C. Gascoyne, Meas. Sci. Technol. 9 (1998) 518–529.